Applied Catalysis A: General 445–446 (2012) 159–165

Contents lists available at SciVerse ScienceDirect

Applied Catalysis A: General

journal homepage: www.elsevier.com/locate/apcata

Photoactivity of S-doped nanoporous activated carbons: A new perspective for harvesting solar energy on carbon-based semiconductors

Teresa J. Bandosz[a,**], Juan Matos[b,*], Mykola Seredych[a], M.S.Z. Islam[c], R. Alfano[c]

[a] Department of Chemistry and CUNY Energy Institute, The City College of New York, 160 Convent Ave, New York, NY 10031, United States
[b] Engineering of Materials and Nanotechnology Centre, Venezuelan Institute for Scientific Research (IVIC), 20632, Caracas 1020-A, Venezuela
[c] Department of Physics, IUIL, The City College of New York, 160 Convent Ave, New York, NY 10031, United States

ARTICLE INFO

Article history:
Received 5 June 2012
Received in revised form 13 August 2012
Accepted 14 August 2012
Available online 25 August 2012

Keywords:
S-doped activated carbon
Photoactivity
Photocurrent
Photocatalysis

ABSTRACT

Photoactivity of S-doped nanoporous carbons was tested using photocurrent generation, cyclic voltammetry and photodegradation of methylene blue (MB) under artificial solar irradiation. The results were compared to those obtained on unmodified carbons and on commercial TiO_2. A significant generation of photocurrent at visible and NIR radiation from 400 to 1200 nm was found. An exposure to ambient light has a strong effect on an open circuit potential indicating the strong activity of S-doped carbons in oxidation reactions. The activity in the process of MB degradation was about 2.2 and 1.9 higher than that obtained on a commercial TiO_2. The extent of photoactivity depends both on the composition of the activated carbon and on the sulfur content. The results suggest that incorporation of sulfur decreases the energy band gap in activated carbon.

1. Introduction

The sun energy harvesting and its technological usage are one of the challenges of contemporary science and engineering [1,2]. Solar energy is produced by photovoltaic devices using semiconductor-based materials such as silicon, carbon, titanium dioxide or zinc oxides. Semiconductors and quantum dots of specific band gap energy are widely explored in order to increase the quantum efficiency of energy conversion [1]. Even though an activated carbon addition to titanium oxide has been studied previously with the intention to enhance the charge separation and decrease the particle size of the semiconductor [3–6], recent developments in graphene science directed the attention of scientist to graphene-semiconductor composites as photocatalysts for solar energy conversion and visible light water splitting reactions [7–10]. Recently Yeh et al. reported the semiconductor properties of graphene oxide (GO) and their application to hydrogen production from water splitting process [11]. The photoactivity of GO was linked to its high dispersion in water and the presence of oxygen groups. Some unspecified groups, not reduced during irradiation process were suggested as responsible for a sustained gap width. That initial band gap was evaluated to be between 2.4 and 4.3 eV. The catalytic properties of activated carbons toward formation of oxygen superions taking an important part in oxidation reactions were investigated by Strelko et al. [12] and Matzer and Boehm [13]. Theoretical calculations indicated that incorporation of certain nitrogen or phosphorus groups decreases the energy gap from 4.8 to 2.88 eV and thus increases the catalytic reactivity of carbons. One of the important applications of this catalytic activity, which can only gain from engagement of photoactivity, is degradation of organic contaminants on activated carbons. Up to now TiO_2 is the best photocatalyst, however it is only photoactive under UV irradiation, which clearly limits its usage in water photodetoxification under real solar conditions [14]. Previous studies have shown that an introduction of oxygen groups to carbon surfaces not only plays a photo-assisting role and enhances TiO_2 photoactivity in the degradations of various organic contaminants [15–19] but also enhances hydrogen photoproduction by water splitting [20] under artificial solar conditions. Recently, the direct photoactivity of activated carbons in UV range was reported by Velasco et al. [21]. Also, Wang et al. [22] and Zhang et al. [23] have showed that graphitic carbon nitrides structures are photoactive under visible light for the hydrogen evolution. Selective oxidation of benzene to phenol was investigated on this kind of materials by Chen et al. [24]. Although a possible decrease in the energy gap caused by introduction of sulfur heteroatoms to a carbon matrix has been hypothesized by Strelko et al. [12], to the best of our knowledge, the present work is the first report on the direct semiconductor photoactivity in visible light of sulfur-doped activated carbons. Very high activity of these kind of carbons for oxidation reactions of ammonia [25] or arsine [26] was reported previously and the activation of oxygen to superoxygen ions as active species

* Corresponding author. Tel.: +58 212 5041166; fax: +58 212 5041166.
** Corresponding author. Tel.: +1 212 6506017.
E-mail addresses: tbandosz@sci.ccny.cuny.edu (T.J. Bandosz), jmatos@ivic.gob.ve, jmatoslale@gmail.com (J. Matos).

0926-860X/$ – see front matter © 2012 Elsevier B.V. All rights reserved.
http://dx.doi.org/10.1016/j.apcata.2012.08.020

in these surface oxidation reactions was hypothesized. Having this in mind, a direct proof of the photoactivity of S-doped carbon is presented in this communication. It is based on the analysis of their capability for photocurrent generation, of photoelectrochemical performance and of the photodegradation of methylene blue (MB) under artificial solar irradiation.

2. Experimental

2.1. Materials and synthesis of S-doped carbons

Two as-received carbons and their sulfur-doped counterparts are analyzed in this work. Their properties were described in detail elsewhere [27,28]. The initial carbons are referred as B (BAX-1500 commercial Mead Westvaco) and C (home-made from polymeric salt [29]), respectively and their sulfur doped counterparts as B-S and C-S. For comparative reasons TiO_2 P25 (Degussa) was employed as photocatalyst [15–20].

2.2. Characterization

Nitrogen adsorption isotherms were measured on ASAP 2010 and surface areas (S_{BET}), micropore volume (V_{mic}), mesopore volume (V_{mes}), total pore volume (V_t) and pore size distributions (PSDs) were calculated [27,28]. The system used to measure the photocurrent is described by Zhang et al. [30]. The photocurrent spectra were measured using white light from Quartz Tungsten Halogen lamp with a computerized Triax 320 monochromator. Selected wavelengths from 300 to 1300 nm were focused into the samples pellets to a spot size of 3.3 mm. Photocurrent was recorded using a Keithley 236 and the power was measured with a Newport 1836 power meter. Cyclic voltammograms were measured in a three-electrode cell with Ag/AgCl as a reference electrode in visible light without any significant optimization of the photons energy. 0.5 M Na_2SO_4 was used as electrolyte with the scan rate of 5 mV/s. The electrodes were prepared [31] by forming a suspension of the carbon materials with polyvinylidene fluoride (PVDF) and commercial carbon black (carbon black, acetylene, 50% compressed, Alfa Aesar) (8:1:1).

2.3. Photocatalytic tests

Photodegradation of methylene blue (MB) was evaluated in a batch photoreactor (open to air cylindrical flask made of Pyrex with a bottom optical window of 6 cm diameter [18]). Irradiation was provided with a metal halide lamp. Photons flux of the lamp was 1.44×10^{17} photons cm^{-2} s^{-1} (90% in the visible region). Irradiation was filtered by a circulating water cell (thickness 2.0 cm) to remove IR beams thus preventing any heating of the suspension. Samples were held in dark for 60 min to reach adsorption equilibrium before irradiation. Photocatalytic tests were performed at 25 °C with samples dispersed in 125 mL of 25 ppm (78.2 μmol/L) methylene blue solution (MB). Kinetic of photodegradation (Fig. 3) was measured for 4–6 h, depending on the sample. After centrifugation (2000 rpm, 5 min) MB aliquots (2.0 mL) were filtered and analyzed by UV-spectrophotometer at 664 nm (Perkin Elmer, λ-35).

3. Results and discussion

3.1. Characterization

3.1.1. Porous structure and surface chemistry

The important information about porosity and surface chemistry is summarized in Table 1 and Fig. 1. The results indicate that

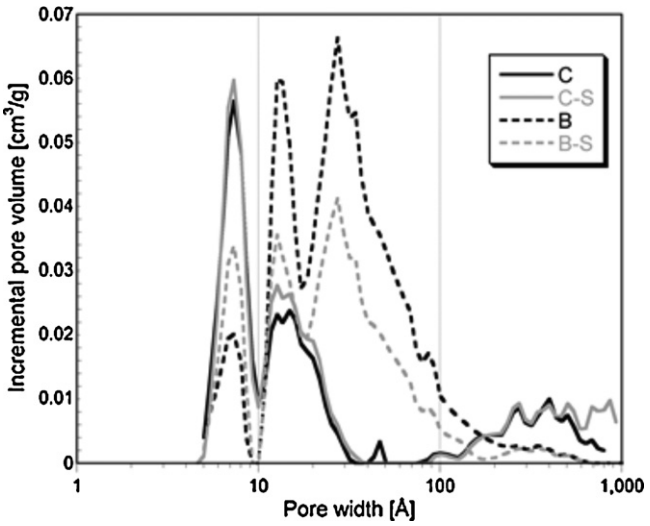

Fig. 1. Pore size distributions of the carbons studied.

C carbons are more microporous than the B samples and that the treatment with sulfur did not change significantly the porosity of the C sample. On the other hand, the porosity of the B sample is affected significantly. After the incorporation of sulfur the volume of pores smaller than 10 Å significantly increased while the volume of mesopores decreased (Fig. 1). During the treatment applied some oxygen groups were decomposed giving free active sites for sulfur incorporation [27,28]. Moreover, the aromaticity of the B-S carbon increased after the doping process since the B sample was manufactured at low temperature (~600 °C while the treatment with H_2S was at 800 °C). XPS analysis [25,29] indicated that in the case of the C-S carbon sulfur is mainly in thiophenic configurations. It is important to mention that a small amount and thus highly dispersed sulfur is also present in the C carbon but the majority of sulfur species is in sulfonic acid functional groups [25,29]. They are responsible for acidity of this carbon and may also contribute to its reactivity under irradiation in a similar manner as reported elsewhere by Matos et al. for the case of oxygenated functional groups [15,17].

3.1.2. Photocurrent measurements

The magnitude of photocurrent generation as a function of λ in our materials upon direct irradiation is presented in Fig. 2. As

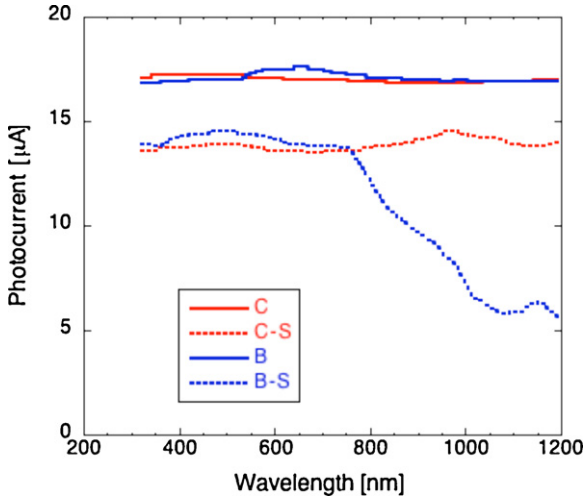

Fig. 2. Photocurrent generated by the carbons studied.

Table 1
Parameters of porous structure and surface chemistry for the carbons studied.

Sample	S_{BET} (m^2/g)	V_t (cm^3/g)	V_{mes} (cm^3/g)	V_{mic} (cm^3/g)	C (%)	O[a] (%)	S (%)	S1[b] (%)	S2[c] (%)	pH
C	1287	0.902	0.433	0.419	88	11	0.8	50	50	4.7
C-S	1354	0.945	0.455	0.490	92	5	3.1	73	27	7.8
B	2053	1.520	1.072	0.449	74	22.6	0	NA	NA	7.0
B-S	1500	1.048	0.672	0.376	90	6.5	2.1	NA	NA	7.3

NA: not analyzed.
[a] B series carbons contain about 1 wt% phosphorus [27].
[b] Contribution of at.% of sulfur in thiophenic species.
[c] Contribution of at.% of sulfur in oxidized species (sulfoxides, sulfone, sulfonic acids).

seen all samples exhibit the photoactivity and the generation of the current is detected in the whole spectral range. When the experiment was done with blocked light no current was detected. That extent of photoactivity was found to decrease when the experiments were repeated with half an hour intervals. Interestingly, after longer time intervals (days) the magnitude of photocurrent generated increased, although it remained lower than that reported initially. Even though these experimental results suggest some instability of carbons under irradiation, which was in fact expected taking into account their reactivity in ambient air [27,28], the flat photocurrent response and the time related recovery are an interesting aspects worth of further study. In the experimental set up used in our study the magnitude of photocurrent cannot be directly linked to the extent of photoactivity since other factors such as the speed of the electron–hole recombination process, conductivity of the materials and density of the pellets and the light absorbing character play a role. Here we use the data collected in Fig. 2 to directly show the ability of our carbons to generate the current in the whole irradiation energy range. This is in contrast to the reference solar cell where the maximum of photoactivity is usually observed in the spectral range. This is also a case for titania whose photoactivity exhibits a maximum at 530 nm in a visible light range and is dependent on the sizes of the particles [32]. Interestingly, the photoactivity for B carbon exhibit a different behavior than those for other samples studied. It is least affected by the time interval between the exposures. All other samples containing sulfur show the much stronger effect, especially B-S. This must be explained by light trapping in their pores where sulfur functional groups are present along with the oxygen. Generation of holes and electrons, besides contributing to the measured current also affects surface chemistry. Some electrons likely reduce oxygen groups, whereas holes may contribute to oxidation, especially when water is present in the pores, which is usually a case in ambient air. Moreover, if sulfur is able to activate oxygen, as suggested previously [27,28], and thus causes formation of superoxygen ions, holes should take part in their oxidation. This process, although crucial for photocatalysis, must limit the extent of photocurrent measured, especially when the conductivity is limited and this should be expected in carbons with high content of heteroatoms. When irradiation is stopped and the carbons are exposed only to ambient air, those freshly reduced surface centers are more active for oxidation by ambient oxygen. In such a process the partial recovery is achieved. This suggests that both, sulfur and oxygen might have a complex contribution to visible light activity of carbonaceous materials. To test this, the activity in the confined space of nanopores where those holes and electrons are trapped owing to limited conductivity of carbons should be analyzed and the results of such tests are addressed below.

3.1.3. Cyclic voltammetry

The comparison of cyclic voltammograms for all samples studied is presented in Fig. 3. 0.5 M Na_2SO_4 was used as electrolyte with the scan rate of 5 mV/s. As seen, significant differences in the photoelectrochemical performance exist. The comparison of the capacitance charge stored values is presented in Fig. 3d. The introduction of sulfur alters the charge storage capability and interestingly, no clear trend can be established and two series of samples exhibit the opposite behavior. While incorporation of sulfur to the C sample decreases its capacitance, an increase is noticed in the case of the B-S sample. Since the charge storage in carbons is a complex phenomenon involving their porosity, chemistry, location of functional groups, pore size distribution and conductivity [31,33] and those features certainly change after the treatment, the analyses of the capacitive behavior were beyond the scope of this communication. The stability of the system can also play a role here. Therefore for the purpose of this analysis we will take a close look on the shape of the CV curves. Here differences are seen in the extent of Faradaic redox reactions represented as humps on CV curves. Although these humps are not expected in neutral electrolyte [34] their existence indicates occurrence of surface reactions [33], not necessary with the involvement of the electrolyte. While for the S-doped carbons the humps are more pronounced in dark, for the C and B carbons the humps are more pronounced when experiments were performed in the light. Those redox processes likely involve surface functional groups and they have their contribution to the capacitance measured. It is possible that either pyrone functionalities or quinone/hydroquinone formation [35,36], especially in the case of the untreated samples, or oxidation/reduction of some thioles/sulfoxides (sulfones, sulfonic acids) takes place. The question why these processes are suppressed in light on S-doped carbons needs to be answered and the answer is likely in the generation of electron–hole pairs in these materials upon visible light exposure. The holes likely recombine with the charge generated upon the potential increase and thus limit the surface redox reactions. The electrons, besides reduction of surface groups can contribute to the activation of the chemisorbed oxygen [12,13]. This may lead to a lower capability for the charge storage as found for C-S. On the other hand, this recombination process does not take place in sulfur-free carbon and therefore the pseudocapacitance contribution is higher in visible light on this material. The explanation of the much higher capacitance on B carbon in light than in dark (much less difference exists for C carbon) is still an open question. Over a 30% increase in the capacitance in light compared to dark can be only explained by an increase in pore accessibility or a decrease in a diffusion limitation for ions. This carbon contains a significant quantity of oxygen (Table 1) and is very susceptible for oxidation [37]. It is possible that active oxygen formed during light exposure and/or holes oxidized the surface, some functional groups are removed as CO_2 (bubbles were noticed at the electrode) and the pores become more accessible. A higher capacitance measured in light on the C-S carbon than in dark is attributed to photogeneration of charge promoted by sulfur species. An opposite effect found for B-S where light decreases the capacitance must be attributed to much greater pseudocapacitance of this carbon compared to C-S seen as intense humps on the CV curves. That pseudocapacitance might decrease when sample is exposed to light as a result of reduction of the oxygen groups by photogenerated electrons and recombination of electron and holes in light results in an apparent decrease in charge

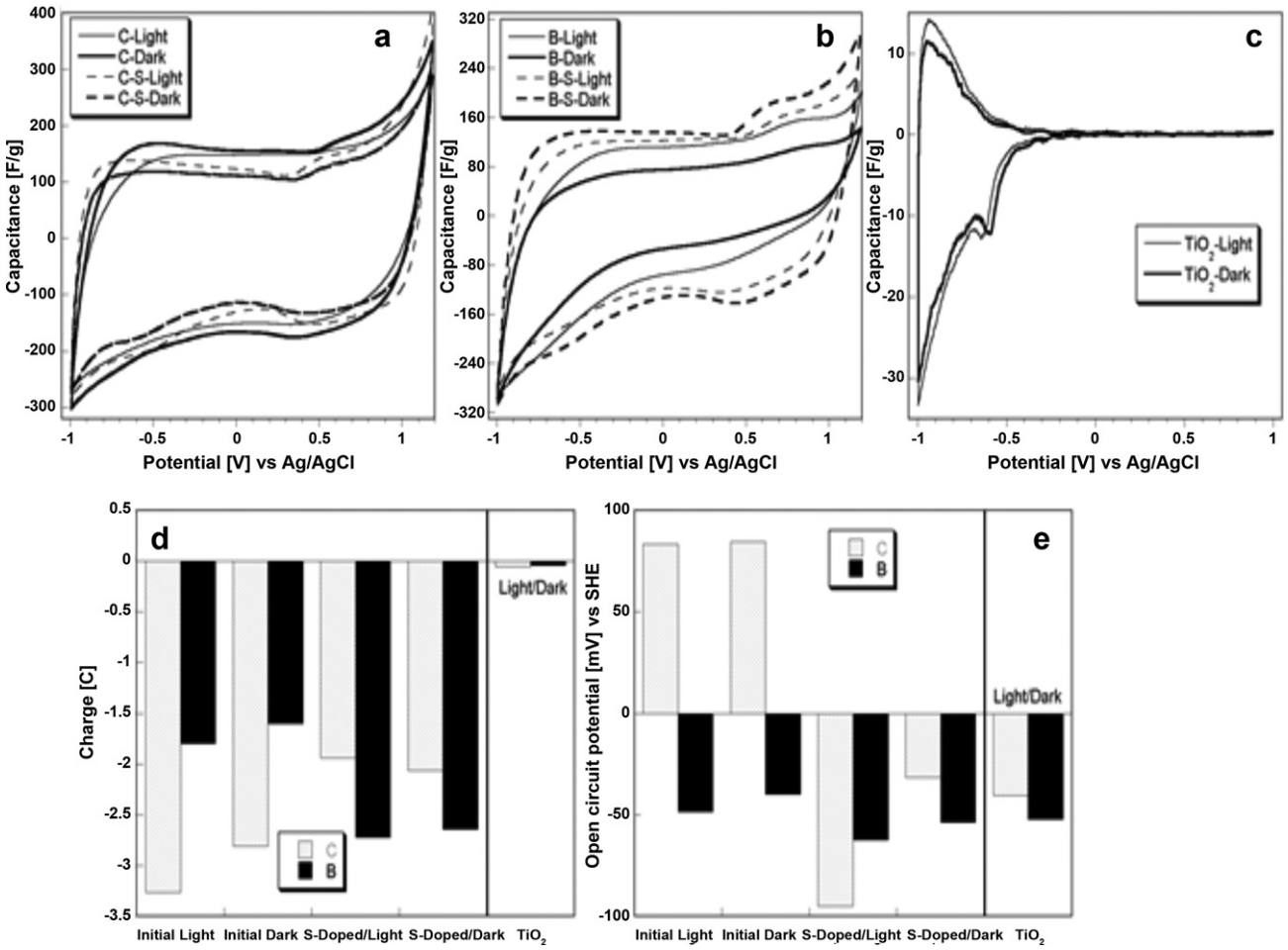

Fig. 3. (a) The CV curves for the C series of samples; (b) the CV curves for the B series of samples; (c) the CV curves for titania P25; (d) comparison of the charge generated on all samples during the CV measurements; (e) comparison of the open circuit current potential.

storage. In the case of titanium dioxide (Fig. 3c) a typical CVs curves are obtained [38–40] with a slight increase in the magnitude of current generated in light. As expected, the capacitance values are very low compared to the carbons owing to small surface area.

The comparison of the open circuit potential (OCP) vs SHE measured in dark and light is presented in Fig. 3e. Only for the initial C carbon the positive values were measured. This carbon significantly differs in surface chemistry from other carbons and exhibits quite acidic surface (Table 1). The negative values obtained for other carbons and titanium dioxide indicate that they work as anodes vs SHE and oxidation reactions are expected to take place. Even though the effect of the light exposure on OCP of P25 titanium dioxide is noticed, it is rather small and light increases the measured OCP (it is slightly less negative than that in dark). The most negative values are found in light for carbons containing sulfur with the most dramatic effect for the C-S carbon. For this material also the difference of OCP in light and in dark is the largest, which suggests it highest photoactivity. For the B-S sample also a decrease in OCP is found in light but it is much less pronounced than that for the C series of samples. Interestingly, when the pH values of the solution before and after ten CV cycles were compared a significant increase in the pH, 1.1 units was found for the C-S carbon measured in light. That increase for B-S was 0.89 units. Increases in dark were only 0.69 and 0.67 unit for C-S and B-S, respectively. This suggests involvement of the electrolyte in redox reactions taking place in visible light. It is likely caused by reduction of sulfur by electrons generated in the system. This might suggest that holes contributed to another process as oxidation of water or/and oxidation of carbon surface.

3.1.4. MB adsorption in the dark and photodegradation

Preliminary adsorption experiments were performed in dark to determine the weights of samples, which should be used to obtain comparable amounts of MB adsorbed in order to compare correctly the photocatalytic activity discussed below. These weights were 6.3 mg for activated carbons and 62.5 mg for TiO_2 and the differences are related to the porosity of materials and their ability to interact with MB. Fig. 4a shows the kinetics of MB adsorption in the dark. The initial rate of adsorption of MB on TiO_2 (P25 from Degussa) (0.254 μmol min^{-1}) is clearly higher than those obtained on other samples. Interestingly, even though about 6 wt% oxygen is present in the S-doped carbons (Table 1) they appear to be extremely hydrophobic materials. This initial trend is consistent with observed very high hydrophobicity of the S-doped carbons as opposite to well-known hydrophilicity of titanium dioxide [41]. The C sample is also quite hydrophilic owing to the presence of sulfonic groups. For hydrophobic carbons with the high sulfur contents, the results suggest that an increase in the sulfur content and in the surface pH have a positive effect on the rate of adsorption. It can be seen from Fig. 4a that after 60 min of the dark exposure to MB equilibrium was reached with the amounts adsorbed of about 36%, 13%, 28%, 20%, and 22% for C, B, C-S, B-S, and TiO_2, respectively. It can be noted from Fig. 4a that most of kinetic of adsorption in the dark have achieved the equilibrium after 60 min because no change in the concentration of MB is detected between 60 and 90 min. The only exception to this was the B-S sample which only adsorbed 2% more MB between 60 and 90 min. However, this very low adsorption value did not affect the kinetic of photodegradation (discussed

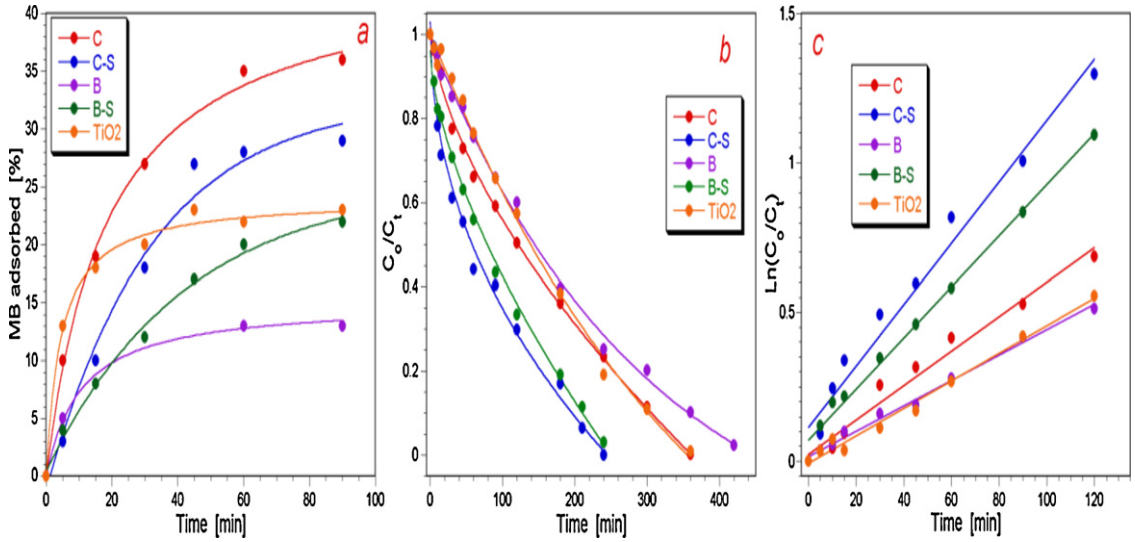

Fig. 4. (a) Kinetics of methylene blue adsorption in the dark; (b) kinetics of MB photodegradation under irradiation with artificial visible light; (c) linear regression from data from (b).

below), because it can be seen from Fig. 4b that in the first 5 min of irradiation, the B-S sample showed about 11% of MB conversion. In short, 11% of MB degradation in only 5 min of irradiation means about 100 times higher MB disappearance than 2% of MB adsorption between 60 and 90 min of adsorption.

Per unit mass all activated carbons adsorbed much more MB than TiO_2-P25 which was expected taking into account the differences in a surface area and porosity (S_{BET} for TiO_2-P25 is about 50 m^2/g [41]). Even though the surface of B-S is higher than of C-S the volume of micropores for the latter sample is higher and thus is the amount of MB adsorbed. Interestingly the ratio of the amount of MB adsorbed on both carbons follows the ratio in the volumes of micropores, ~1.3. This is explained by well-known phenomenon of the overlapping of the adsorption potential in pores similar in size to adsorbate molecule [42]. The small amount adsorbed on the B sample can be explained by its high content of oxygen blocking the access of MB to small pores and also creating the hindrance for its more energetically favorable position on the surface. On the other hand, the large amount adsorbed on the C carbon compared to C-S, even though their porosity is similar can be linked to surface acidity, MB has a basic nature and it is expected to be stronger attracted to acidic sites.

When the photodegradation of MB was carried out at the same conditions without the presence of the photoactive solid [17,18] a direct photolysis was negligible. Fig. 4b shows the kinetics of MB photodegradation when the carbons and titania are present in the system. In Fig. 4c the linear regression of the kinetic data is presented. A summary of the kinetic results for the photodegradation of MB such as initial rate (v_o), relative initial activity (v_{rel}), apparent first-order rate constant (k_{app}), and photoactivity (ϕ_{photo}) is included in Table 2. The results suggest that C-S is slightly more photoactive than B-S and both of them are clearly more photoactive than TiO_2 alone. Even the C sample, which contains 0.8% sulfur, is found to be more photoactive than TiO_2. Total disappearance of MB from solutions with dispersed S-doped carbons is found after 4 h while TiO_2 requires at least about 6 h. It has to be mentioned here the kinetic experiments in dark showed the comparable efficiency of MB removal on all three sulfur containing samples and titania (20–36%). Previous results obtained at the same experimental conditions on non-doped home-made activated carbons of similar porosity to that of the carbons studied here [17] showed a lack of photoactivity for MB degradation under the same artificial solar light. Our results demonstrate that both S-doped AC are photoactive and this photoactivity is even higher than that of TiO_2. Comparison of the kinetics results in Table 2 shows that initial rates (v_o) on C-S and B-S are 2.1 and 1.9 higher relative to that found for TiO_2. In addition, it should be also pointed out here that considering the apparent first-order rate constant (k_{app}) estimated from the first 2 h of reaction, the photoactivity (ϕ_{photo}) of the C-S and B-S samples are 2.2 and 1.9 higher compared to that of TiO_2. The main intermediate products of MB photodegradation were previously reported by Herrmann and co-workers [43]. In addition, the similarity between v_{rel} and ϕ_{photo} values (Table 2) indicates that the intermediates formed during the degradation reaction do not affect the photoactivity of the S-doped carbons. This is a consequence of the capability of S-doped carbons to adsorb continuously basic organic compounds such as MB, as discussed above. A similar behavior was reported for the consecutive photocatalytic runs during the phenol photodegradation on a binary TiO_2-activated carbon catalyst [44] where intermediates produced during reaction only affect lightly the photoactivity after the third photocatalytic run. Since there is no diffusion limitation for the MB adsorption from solution to the AC surface, photoactivity is not affected during reaction or in other words, photocatalyst is not deactivated during reaction [44].

3.1.5. General discussion

An activated carbon consists of a complex matrix, and in spite of the fact that the higher sulfur content apparently results in higher photoactivity, this photoactivity is affected not only by S contents, but also by the pore size distribution and surface pH [14–20]. The latter is strongly affected by the oxygen content. We do believe that surface pH and pore size distribution affect the photoactivity because photoreactions can occur both on the surface and within the pores, especially those of small sizes. These micropores, besides being able to absorb photons and to work as unique microreactors for their complex chemical activity involving electron–hole formation, are able to capture the intermediates formed during reaction [44]. Thus photodegradation of the intermediates can take place at the same sites where they are formed without a complex diffusion to the surface. In this process, the limited electric conductivity of the carbon matrix discussed above can be a plus.

We suggest that sulfur functional organic groups such as sulfur in aromatic rings, sulfoxides, sulfones [45] are responsible the photoactivity of the S-doped activated carbon. The materials work

Table 2
Summary of kinetic results for the MB photodegradation.

Sample	v_o [a] (μmol L^{-1} min^{-1})	v_{rel} [b]	$k_{app} \times 10^{-3}$ [c] (min^{-1})	R[d]	ϕ_{photo} [e]
C (6.3 mg)	0.291	1.04	6.00	0.97400	1.3
C-S (6.3 mg)	0.579	2.1	10.28	0.96932	2.2
B (6.3 mg)	0.262	0.93	4.00	0.98700	0.87
B-S (6.3 mg)	0.536	1.9	8.56	0.99165	1.9
TiO_2 (62.5 mg)	0.281	1.0	4.61	0.98487	1.0

[a] Initial rate estimated from $C_{eq} \cdot k_{app}$, where, C_{eq} is the MB concentration in solution after achieving the equilibrium of adsorption in the dark.
[b] Relative initial activity obtained from $v_{o\text{-}AC}/v_{o\text{-}TiO_2}$.
[c] Apparent first-order rate constant for the MB photodegradation (k_{app}).
[d] Square regression factor obtained from OriginLab statistics (R-square).
[e] ϕ_{photo} defined as the photoactivity relative to TiO_2 obtained from $k_{app\text{-}AC}/k_{app\text{-}TiO_2}$.

apparently better than titania. Their black nature and hydrophobicity cause that all the visible energy is harvested in the pore system. Incorporation of sulfur likely decreases the band gap and electron–hole pairs are formed. The physics of band-gap shrinkage in materials, ranging from nano-crystals to nano-composites have been investigated [46–52]. It is widely accepted that band-gap shrinkages occur due to electron–impurity interactions as well as Coulomb-interaction between carriers. Grein and John [52] suggested that the interaction between electron and acoustic-phonon as well as interaction between electron and static-disorder results are responsible for downshift of the band-gap. The impurities and heterojunctions in our case are those linked to sulfur doping. The phonon-confinement in the small pores sizes can also play an important role in downshifting the band-gap energies in S-doped carbon. The limited conductivity of carbon phase promotes charge transfer and its hydrophobic nature results in a strong attraction of organic species. Their degradation can occur via electron transfers from the molecule to the surface where hole is located. Electrons generated likely help in this via activation of oxygen, which should significantly contribute the degradation of adsorbates. However, elimination of oxygen in this process can have negative effect on the generation of active oxygen farther participating in oxidation reactions. This process reflects in the parabolic curves representing the kinetics of photodegradation.

4. Conclusions

The present results have a potential to open a new path for energy harvesting technology where inexpensive and easily produced materials, S-doped activated carbons can be used. The present results suggest that photocatalyst in visible light can be optimized to reduce the costs of energy consumption. The photocurrent results indicate that both, sulfur and oxygen have a complex contribution to visible light activity of carbonaceous materials. The CV studies imply that holes in sulfur-doped carbons contributed to oxidation of water or/and oxidation of carbon surface. Obviously, the stability of activated carbons upon irradiation can be a problem but this issue can be addressed by detailed study directed toward the stability of their surface upon oxidation. This can be achieved by inactivation/saturation of their surface centers contributing to redox reactions. Its black character helps in harvesting solar spectrum, electron–hole pairs are formed and limited electric conductivity traps charge in the porous structure. Thus, a system of unique nanoreactors is formed as suggested by the clear increase in the photoactivity for the degradation of MB in comparison to commercial TiO_2. The extent of the study toward DC conductivity improvement depends on the target application. Apparently for energy harvesting conductivity should be increased increasing the graphitization level but for the photocatalytic processes trapping generated electrons and holes in the pore system can be a plus.

Acknowledgments

This work was supported in part by IUSL internal funds provided by Venezuelan Ministry of Science and Technology. TJB research was funded ARO (W911NF-10-1-0039) and NSF (CBET 0754945/0754979 and CET 1133112).

References

[1] R.M. Navarro Yerga, M.C. Alvarez-Galvan, F. Del Valle, J.A. Villoria de la Mano, J.L.G. Fierro, ChemSusChem 2 (2009) 471–485.
[2] V. Balzani, A. Credi, M. Venture, ChemSusChem 1 (2008) 26–58.
[3] C. Pelekani, V.L. Snoeyink, Carbon 38 (2000) 1423–1436.
[4] B. Tryba, A. Morawski, M. Inagaki, M. Toyoda, Appl. Catal. B: Environ. 63 (2006) 215–221.
[5] R.J. White, V. Budarin, R. Luque, J.H. Clark, D.J. Macquarrie, Chem. Soc. Rev. 38 (2009) 3401–3418.
[6] Y. Tao, M. Endo, M. Inagaki, K. Kaneko, J. Mater. Chem. 21 (2011) 313–323.
[7] Y.H. Ng, A. Iwase, A. Kudo, R. Amal, J. Phys. Chem. Lett. 1 (2010) 2607–2612.
[8] Z. Zhan, L. Zheng, Y. Pan, G. Sun, L. Li, J. Mater. Chem. 22 (2012) 2589–2595.
[9] H.B. Yang, C.X. Guo, G.H. Guai, Q.L. Song, S.P. Jiang, C.M. Li, Appl. Mater. Interfaces 3 (2011) 1940–1945.
[10] H. Ma, J. Han, Y. Fu, Y. Song, C. Yu, X. Dong, Appl. Catal. B: Environ. 102 (2011) 417–423.
[11] T.F. Yeh, J.M. Syu, C. Cheng, T.H. Chang, Adv. Funct. Mater. 20 (2010) 2255–2262.
[12] V.V. Strelko, V.S. Kutz, P.A. Thrower, Carbon 38 (2000) 1453–1499.
[13] S. Matzer, H.P. Boehm, Carbon 36 (1998) 1697–1709.
[14] J. Matos, J.M. Chovelon, T. Cordero, C. Ferronato, Open Environ. Eng. J. 2 (2009) 21–29.
[15] J. Matos, A. García, T. Cordero, J.M. Chovelon, C. Ferronato, Catal. Lett. 130 (2009) 568–574.
[16] J. Matos, A. García, P.S. Poon, J. Mater. Sci. 45 (2010) 4934–4944.
[17] J. Matos, A. García, L. Zhao, M.M. Titirici, Appl. Catal. A: Gen. 390 (2010) 175–182.
[18] J. Matos, M. Rosales, A. García, C. Nieto-Delgado, J.R. Rangel-Mendez, Green Chem. 13 (2011) 3431–3439.
[19] J. Matos, E. García-López, L. Palmisano, A. García, G. Marci, Appl. Catal. B: Environ. 99 (2010) 170–180.
[20] J. Matos, T. Marino, R. Molinari, H. García, Appl. Catal. A: Gen. 417 (2012) 263–272.
[21] L.F. Velasco, I.M. Fonseca, J.B. Parra, J.C. Lima, C.O. Ania, Carbon 50 (2012) 249–258.
[22] X. Wang, K. Maeda, X. Chen, K. Takanabe, K. Domen, Y. Hou, X. Fu, M. Antonietti, J. Am. Chem. Soc. 131 (2009) 1680–1681.
[23] J. Zhang, X. Chen, K. Takanabe, K. Maeda, K. Domen, J.D. Epping, X. Fu, M. Antonietti, X. Wang, Angew. Chem. Int. Ed. 49 (2010) 441–444.
[24] X. Chen, J. Zhang, X. Fu, M. Antonietti, X. Wang, J. Am. Chem. Soc. 131 (2009) 11658–11659.
[25] C. Petit, K. Kante, T.J. Bandosz, Carbon 48 (2010) 654–667.
[26] C. Petit, G.W. Peterson, J. Mahle, T.J. Bandosz, Carbon 48 (2010) 1779–1787.
[27] M. Seredych, T.J. Bandosz, Appl. Catal. B: Environ. 106 (2011) 133–141.
[28] M. Seredych, M. Khine, T.J. Bandosz, ChemSusChem 4 (2011) 139–147.
[29] D. Hines, A. Bagreev, T.J. Bandosz, Langmuir 20 (2004) 3388–3397.
[30] S.K. Zhang, H. Ahmar, B. Chen, W. Wang, R. Alfano, Proc. SPIE 7934 (2011), 1A1–1A5.
[31] D. Hulicova-Jurcakova, M. Seredych, G.Q. Lu, N.K.A.C. Kodiweera, P.E. Stallworth, S. Greenbaum, T.J. Bandosz, Carbon 47 (2009) 1576–1584.
[32] G.W. Lee, S.Y. Bang, C. Lee, W.-M. Kim, D. Kim, K. Kim, N.G. Park, Curr. Appl. Phys. 9 (2009) 900–906.
[33] J. Chmiola, G. Yushin, Y. Gogotsi, C. Portet, P. Simon, P.L. Taberna, Science 313 (2006) 1760–1763.
[34] H.A. Andreas, B.E. Conway, Electrochim. Acta 51 (2006) 6510–6520.
[35] E. Frackowiak, G. Lota, J. Machnikowski, C. Vix-Guterl, F. Béguin, Electrochim. Acta 51 (2006) 2209–2214.
[36] M.P. Bichat, E. Raymundo-Pinero, F. Beguin, Carbon 48 (2010) 4351–4361.
[37] I.I. Salame, T.J. Bandosz, Ind. Eng. Chem. Res. 39 (2000) 301–306.

[38] J. Zhang, C. Yang, G. Chang, H. Zhu, M. Oyama, Mater. Chem. Phys. 88 (2004) 398–403.
[39] F. Fabregat-Santiago, I. Mora-Seró, G. Garcia-Belmonte, J. Bisquert, J. Phys. Chem. B 107 (2003) 758–768.
[40] G. Jiang, H. Tang, L. Zhu, J. Zhang, B. Lu, Sens. Actuators B 138 (2009) 607–612.
[41] J. Matos, A. Corma, Appl. Catal. A: Gen. 404 (2011) 103–112.
[42] D.W. Everett, J.C. Powl, J. Chem. Soc., Faraday Trans. 72 (1984) 619–621.
[43] A. Houas, H. Lachheb, M. Ksibi, E. Elaloui, C. Guillard, J.M. Herrmann, Appl. Catal. B: Environ. 31 (2001) 145–157.
[44] J. Matos, J. Laine, J.M. Herrmann, D. Uzcategui, J.L. Brito, Appl. Catal. B: Environ. 70 (2007) 461–469.
[45] A. Samokhvalov, ChemPhysChem 12 (2011) 2870–2885.
[46] M. Kranjcec, I.P. Studenyak, M.V. Kuric, J. Non-Cryst. Solids 355 (2009) 54–57.
[47] X. Chen, L. Liu, P.Y. Yu, S.S. Mao, Science 331 (2011) 746–750.
[48] A.A. Dakhel, Opt. Mater. 31 (2009) 691–695.
[49] A. Naldoni, M. Alliieta, S. Santangelo, M. Marelli, F. Fabbri, S. Cappelli, C.L. Bianchi, R. Psaro, V.D. Santo, J. Am. Chem. Soc. 134 (2012) 7600–7603.
[50] A.P. Roth, J.B. Webb, D.F. Williams, Phys. Rev. B 25 (1982) 7836–7839.
[51] S. Wendt, P.L. Sprunger, E. Lira, G.K.H. Madseon, Z. Li, J. Hansen, J. Matthiesen, A. Blekinge-Rasmussen, E. Laegsgaard, B. Hammer, F. Besenbacher, Science 320 (2008) 1755–1759.
[52] C.H. Grein, S. John, Phys. Rev. B 39 (1989) 1140–1151.